Large anharmonic effect and thermal expansion anisotropy of metal chalcogenides: The case of antimony sulfide

Chee Kwan Gan[*] and Jian Rui Soh

Institute of High Performance Computing, 1 Fusionopolis Way, 16-16 Connexis, Singapore 138632

Yun Liu

Department of Materials Science and Engineering, Massachusetts Institute of Technology,
77 Massachusetts Avenue, Cambridge, Massachusetts 02139, USA

We derive a compact matrix expression for the linear thermal expansion coefficients (TECs) for a general orthorhombic system which relates elastic properties and integrated quantities based on deformation and mode dependent Grüneisen parameters and mode dependent heat capacities. The density of Grüneisen parameters $\Gamma(\nu)$ as a function of frequency ν, weighted by the number of phonon modes, is introduced and found to be illuminating in interpreting the TEC results. Using density functional perturbation theory and Grüneisen formalism for thermal expansion, we illustrate the general usefulness of this method by calculating the linear and volumetric TECs of a low-symmetry orthorhombic compound antimony sulfide (Sb_2S_3), which belongs to a large class of technologically and fundamentally important materials. Even though negative Grüneisen parameters are found for deformations in all three crystal directions, the $\Gamma(\nu)$ data rule out the occurrences of negative TECs at all temperatures. Sb_2S_3 exhibits a large thermal expansion anisotropy where the TEC in the b direction can reach as high as 13×10^{-6} K^{-1} at high temperatures, about two and seven times larger than the TECs in the c and a direction, respectively. Our work suggests a general and practical first-principles approach to calculate the thermal properties of other complicated low-symmetry systems.

I. INTRODUCTION

Metal chalcogenides comprise an important class of semiconductors for optoelectronics, photovoltaics, and thermoelectrics [1–5]. Recently, Raman spectroscopies and pump probe experiments on examples such as Bi_2S_3 and Sb_2S_3 have demonstrated the importance of phonons in modulating fundamental scattering processes [5,6]. Even though phonon dispersions have been reliably obtained for some of these materials [5,7], a first-principles study of the anharmonic effects due to phonon-phonon scatterings that account for thermal conductivities and thermal expansion coefficients (TECs) has been lacking. This could be attributed to the fact that metal chalcogenides have a relatively large primitive cell and a low-symmetry orthorhombic structure with three lattice parameters, in contrast to some of the well-studied cubic structures with a single lattice parameter [8,9]. TECs may routinely be calculated using a direct minimization approach within the quasiharmonic approximation [10]. However, for metal chalcogenides, huge computational costs are needed to perform many phonon calculations to locate a free-energy minimum at a given temperature in the three-dimensional lattice parameter space. Moreover, even if a direct minimization approach could be carried out, it may be difficult to understand the underlying physics without investigating fundamental quantities such as the Grüneisen parameters, elastic constants, heat capacities, and mean-square displacements (MSDs).

Here we should mention a recent first-principles approach that is based on the vibrational self-consistent-field to calculate TECs [11]. In another work [12], a nonequilibrium Green's-function method is used to calculate TECs of carbon nanotubes and graphene with a force-field potential.

II. METHODOLOGY

In this paper we adopt the Grüneisen formalism [13–15] to predict the thermal properties of a low-symmetry orthorhombic system with a first-principles method. To the best of our knowledge it is the first time a first-principles thermal expansion study has been done on a crystal that is characterized by three lattice parameters. We find that the linear TECs of an orthorhombic system in the a, b, and c directions, denoted by α_1, α_2, and α_3, respectively, at a temperature T may be described by a matrix equation:

$$\alpha = \frac{1}{\Omega} C^{-1} I, \tag{1}$$

where $\alpha^T = (\alpha_1, \alpha_2, \alpha_3)$, Ω is the equilibrium volume of the primitive cell, and C^{-1} is the elastic compliance matrix [16] with matrix elements C_{ij} being the elastic constants. A component $I_i(T)$ of the vector $I = (I_1, I_2, I_3)^T$ is given by $I_i(T) = \frac{\Omega}{(2\pi)^3} \sum_\lambda \int_{BZ} \gamma_{i,\lambda k} c(\nu_{\lambda k}, T) \, dk$ where the integral is over the first Brillouin zone (BZ). A phonon mode with frequency $\nu_{\lambda k}$ is labeled by a mode index λ and a wave vector k. The heat capacity of a phonon mode with frequency ν at temperature T is $c(\nu, T) = k_B r^2 / \sinh^2 r$, with $r = h\nu/2k_B T$. h and k_B are the Planck and Boltzmann constants, respectively. The mode Grüneisen parameters $\gamma_{i,\lambda k} = -\nu_{\lambda k}^{-1} \partial \nu_{\lambda k}/\partial \epsilon_i$ measure the relative change of phonon frequencies $\nu_{\lambda k}$ as a result of deformations applied to the crystal characterized by strain parameters ϵ_i.

To illustrate the usefulness of our method, we carry out density functional theory calculations using the plane-wave

*Corresponding author: ganck@ihpc.a-star.edu.sg

basis QUANTUM ESPRESSO suite [17] on Sb_2S_3, an example of metal chalcogenides with a small direct band gap of 1.5 eV. The local-density approximation is used to describe the exchange correlation. Pseudopotentials based on the Rappe-Rabe-Kaxiras-Joannopoulos [18] approach as found in the "atomic code" of the standard QUANTUM ESPRESSO distribution are used. A large cutoff energy of 60 Ry is used throughout and a Monkhorst-Pack mesh of $4 \times 12 \times 4$ is used for k-point sampling. Atomic relaxation is stopped when the forces on all the atoms are less than 1 meV/Å. We use the nonsymmorphic space group *Pnma* to describe Sb_2S_3 with 20 atoms in a primitive cell, of which 5 are inequivalent. We obtain $a_0 = 11.021$ Å, $b_0 = 3.797$ Å, and $c_0 = 10.783$ Å, in good agreement with experimental values [19]. The phonon modes are calculated using the density functional perturbation theory [20]. Phonon calculations are carried out on a q mesh of $2 \times 4 \times 2$, which is equivalent to a $2 \times 4 \times 2$ supercell force-constant [21] phonon calculation, the efficacy of which has been confirmed [7]. We note that the results do not appreciably change when we use a larger q mesh of $3 \times 6 \times 3$. For the q mesh of $2 \times 4 \times 2$, dynamical matrices have to be calculated at 12 irreducible q points. For a general q point, one has to loop through 60 irreducible representations, each of which requires a number of self-consistent-field calculations. Interestingly, the seemingly high-symmetry point Γ has a relatively large number of irreducible representations of 60, which incurs more computation costs compared to, say, a diamond crystal with only 2 irreducible representations at Γ. The 12-q points correspond to a total of 471 irreducible representations. Ignoring the cost for convergence tests, we already need to handle a minimum of $7 \times 471 = 3297$ irreducible representations to carry out a central-difference scheme for a, b, and c directions (note that we need to perform a set of phonon calculations on the equilibrium structure). The cost analysis also suggests even larger computational resources will be required if one wishes to carry out a full direct minimization study based on the quasiharmonic approximation in finding the free-energy minimum at each temperature in the three-dimensional search space of $\{a,b,c\}$. At the end of self-consistent-consistent calculations, all dynamical matrices are collected and interatomic force constants are obtained by an inverse Fourier transform. The Brillouin-zone sampling for the integrated quantities $I_i(T)$ is over a large mesh of $15 \times 45 \times 15$. We perform standard elastic constants calculations [22,23] to obtain $(C_{11}, C_{12}, C_{13}, C_{22}, C_{23}, C_{33}) = (133.19, 36.45, 55.99, 141.08, 67.14, 119.09)$ GPa.

III. RESULTS AND DISCUSSIONS

We apply strains of $\epsilon = \pm 0.005$ (strains of $\epsilon = \pm 0.010$ do not change the results appreciably) to obtain the central-difference Grüneisen parameters in the a, b, and c directions. By using the change in the dynamical matrix resulting from a finite deformation to the crystal and with the help of first-order perturbation theory, we can determine the change of frequency for each phonon mode to obtain the Grüneisen parameters. The results of $\gamma_{i,\lambda k}$ are shown in Fig. 1. It is noticed that along the high-symmetry directions the degeneracy of the Grüneisen parameters is preserved. There are some bands that have large values (say, >4) of Grüneisen parameters. By performing a
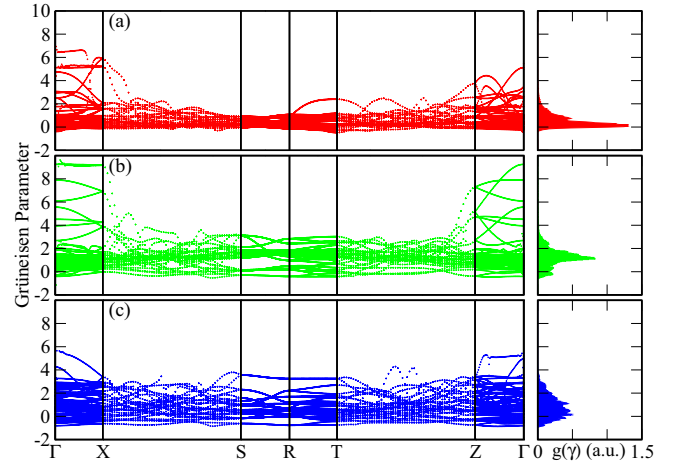

FIG. 1. (Color online) Grüneisen parameters $\gamma_{i,\lambda k}$ along the high-symmetry directions for orthorhombic Sb_2S_3, for $i = 1$, 2, and 3, corresponding to deformations due to strains e_1, e_2, and e_3, are shown in (a), (b), and (c), respectively. The coordinates of X, S, R, T, and Z can be found in Ref. [7]. The corresponding plain densities of Grüneisen parameters are shown on the right.

k-point sampling over the BZ, we calculate the plain density of Grüneisen parameters $g_i(\gamma) = \frac{\Omega}{(2\pi)^3} \sum_\lambda \int_{BZ} \delta(\gamma - \gamma_{i,\lambda k}) \, d\mathbf{k}$, results of which are shown in the right panels of Fig. 1. The $g_i(\gamma)$ plots show that large Grüneisen parameters are not highly populated. Interestingly, $g_i(\gamma)$ show some population of negative Grüneisen parameters, especially for $g_3(\gamma)$, which may lead to negative TECs if these negative parameters correspond to low-frequency modes. In the literature, one can use the average Grüneisen parameters [9] or the scattered γ-ν plot [24] to display this information. However, here we propose a quantity called the density of Grüneisen parameters $\Gamma_i(\nu)$, weighted by the number of phonon modes, defined as $\Gamma_i(\nu) = \frac{\Omega}{(2\pi)^3} \sum_\lambda \int_{BZ} \delta(\nu - \nu_{\lambda k}) \gamma_{i,\lambda k} \, d\mathbf{k}$ to capture the collective effects of Grüneisen parameters and phonon
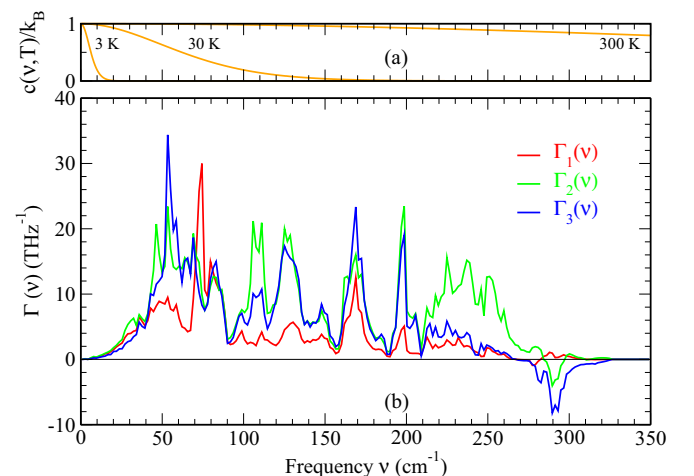

FIG. 2. (Color online) (a) The mode dependent heat capacity as a function of phonon frequency ν for three representative temperatures. (b) Density of Grüneisen parameters.
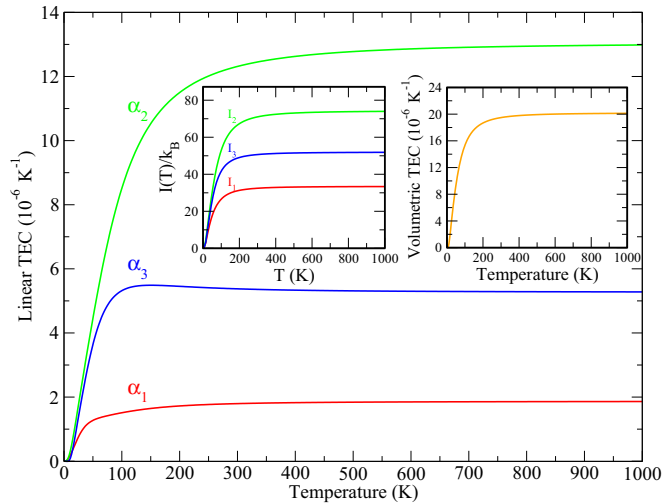
FIG. 3. (Color online) The linear TECs of Sb_2S_3 as functions of temperature. The insets show the integrated quantities $I_i(T)$ and the volumetric TEC.
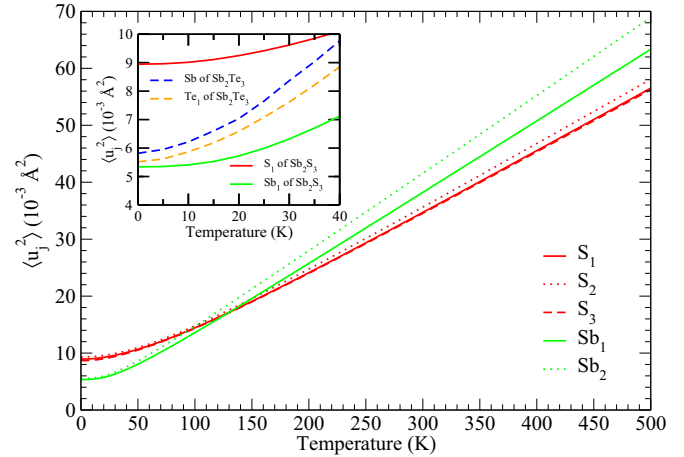

FIG. 4. (Color online) MSDs of five inequivalent atoms of Sb_2S_3 as functions of temperature. The inset shows the comparison of the MSDs of representative atoms in Sb_2S_3 and a reference trigonal system of Sb_2Te_3. The MSD for the jth atom is [25] calculated from $\langle u_j^2 \rangle = \frac{\Omega}{(2\pi)^3} \sum_\lambda \int_{BZ} \frac{h|e_j(\lambda,\boldsymbol{k})|^2 \coth r}{8\pi^2 M_j \nu_{\lambda k}} \, d\boldsymbol{k}$ with $r = h\nu_{\lambda k}/2k_B T$ and $e_j(\lambda,\boldsymbol{k})$ the eigenvector for the jth atom of mass M_j.

frequencies. Apart from its direct physical meaning, $\Gamma_i(\nu)$ also allows a second equivalent expression for $I_i(T)$, which is $\int_{\nu\min}^{\nu\max} \Gamma_i(\nu)c(\nu,T) \, d\nu$. The densities of Grüneisen parameters $\Gamma_i(\nu)$ are shown in Fig. 2(b), where the negative Grüneisen parameters are confined to phonon frequencies of around 290 cm^{-1}. These phonons are not excited at low temperatures [see Fig. 2(a) for the dependence of $c(\nu,T)$ on ν for representative temperatures of 3, 30, and 300 K].

The results of the linear and volumetric thermal expansion coefficients are shown in Fig. 3. Except for α_3 beyond 150 K, all TECs are monotonically increasing functions of temperature. $I_i(T)$ (shown in an inset of Fig. 3) also exhibits a largely similar temperature dependence. Despite the occurrences of negative Grüneisen parameters as shown in Fig. 1, all linear and volumetric TECs are positive. At high temperatures, the effect of phonon modes with negative Grüneisen parameters is canceled out by the more highly populated phonon modes at lower frequencies with positive Grüneisen parameters, thus eliminating the possibility of negative TECs at any temperature. The high-temperature limits are $\alpha_1 = 1.86$, $\alpha_2 = 13.0$, and $\alpha_3 = 5.28 \times 10^{-6} \text{ K}^{-1}$, and the volumetric TEC is $20.14 \times 10^{-6} \text{ K}^{-1}$. The small TEC of α_1 among all other TECs is consistent with the fact that $I_1(T)$ is smaller than $I_2(T)$ and $I_3(T)$, in addition to the fact that C_{11} is comparable to C_{22} but larger than C_{33}. To the best of our knowledge, experimental TEC data of Sb_2S_3 are not readily available for a direct comparison. However, we note that Stoffel *et al.* [24] have demonstrated that the volumetric TEC of trigonal Sb_2Te_3 using a quasiharmonic approximation is accurate up to 300 K where the mean-square displacements (MSDs) of Sb_2Te_3, shown in the inset of Fig. 4, compare rather well with that of Sb_2S_3. Therefore we believe our TEC

results on Sb_2S_3 are reasonable below 40 K. We note that the MSDs of Sb_2Te_3 at higher temperatures (which are not available in Ref. [24]) may provide a better estimate on the temperature below which our TEC results are valid. At low temperatures below 100 K, Fig. 4 shows that the three S atoms have larger MSDs than Sb, consistent with the fact that S has a smaller mass compared to Sb. At high temperatures, however, the MSDs of Sb atoms are larger than that of the S atoms.

IV. SUMMARY

In summary we have extended the Grüneisen formalism to treat a low-symmetry structure of orthorhombic antimony sulfide. Using this approach, we applied just six deformations to the crystal to obtain the Grüneisen parameters, thus avoiding the huge computation requirement for a direct minimization based on the quasiharmonic approximation. Even though negative Grüneisen parameters were found, there are no negative TECs at all temperatures since these parameters are associated with high-frequency modes at around 290 cm^{-1}. It is expected that a similar approach could be used to address TECs of other low-symmetric systems such as those with monoclinic crystal structure.

[1] B. Roy, B. R. Chakraborty, R. Bhattarharya, and A. K. Dutta, Solid State Commun. **25**, 937 (1978).

[2] L. P. Deshmukh, S. G. Holikatti, B. P. Rane, B. M. Moore, and P. P. Hankare, J. Electrochem. Soc. **141**, 1779 (1994).

[3] Y. Porat and R. Y. Ting, Ferroelectrics **87**, 155 (1988).

[4] R. Caracas and X. Gonze, Phys. Chem. Miner. **32**, 295 (2005).

[5] Y. Zhao, Kun Ting Eddie Chua, C. K. Gan, J. Zhang, B. Peng, Z. Peng, and Q. Xiong, Phys. Rev. B **84**, 205330 (2011).

[6] W. K. Chong, G. Xing, Y. Liu, E. L. Gui, Q. Zhang, Q. Xiong, N. Mathews, C. K. Gan, and T. C. Sum, Phys. Rev. B **90**, 035208 (2014).

[7] Y. Liu, Kun Ting Eddie Chua, T. C. Sum, and C. K. Gan, Phys. Chem. Chem. Phys. **16**, 345 (2014).

[8] P. Pavone, K. Karch, O. Schütt, W. Windl, D. Strauch, P. Giannozzi, and S. Baroni, Phys. Rev. B **48**, 3156 (1993).

[9] K.-P. Bohnen, R. Heid, L. Pintschovius, A. Soon, and C. Stampfl, Phys. Rev. B **80**, 134304 (2009).

[10] N. Mounet and N. Marzari, Phys. Rev. B **71**, 205214 (2005).

[11] B. Monserrat, N. D. Drummond, and R. J. Needs, Phys. Rev. B **87**, 144302 (2013).

[12] J.-W. Jiang, J.-S. Wang, and B. Li, Phys. Rev. B **80**, 205429 (2009).

[13] E. Grüneisen, Hand. Phys. **10**, 1 (1926).

[14] T. H. K. Barron, J. G. Collins, and G. K. White, Adv. Phys. **29**, 609 (1980).

[15] P. K. Schelling and P. Keblinski, Phys. Rev. B **68**, 035425 (2003).

[16] C. Kittel, *Introduction to Solid State Physics*, 7th ed. (Wiley, New York, 1996).

[17] P. Giannozzi, S. Baroni, N. Bonini, M. Calandra, R. Car, C. Cavazzoni, D. Ceresoli, G. L. Chiarotti, M. Cococcioni, I. Dabo *et al.*, J. Phys.: Condens. Matter **21**, 395502 (2009).

[18] A. M. Rappe, K. M. Rabe, E. Kaxiras, and J. D. Joannopoulos, Phys. Rev. B **41**, 1227 (1990).

[19] L. F. Lundegaard, R. Miletich, T. Balic-Zunic, and E. Makvicky, Phys. Chem. Miner. **30**, 463 (2003).

[20] S. Baroni, S. de Gironcoli, A. D. Corso, and P. Giannozzi, Rev. Mod. Phys. **73**, 515 (2001).

[21] C. K. Gan, Y. P. Feng, and D. J. Srolovitz, Phys. Rev. B **73**, 235214 (2006).

[22] O. Beckstein, J. E. Klepeis, G. L. W. Hart, and O. Pankratov, Phys. Rev. B **63**, 134112 (2001).

[23] H. Koc, A. M. Mamedov, E. Deligoz, and H. Ozisik, Solid State Sci. **14**, 1211 (2012).

[24] R. P. Stoffel, V. L. Deringer, R. E. Simon, R. P. Hermann, and R. Dronskowski, J. Phys.: Condens. Matter **27**, 085402 (2015).

[25] Y. Yang and Y. Kawazoe, Europhys. Lett. **98**, 66007 (2012).